An anti-diffusive HLL scheme for the electronic M1 model in the diffusion limit

Christophe Chalons, Sébastien Guisset

An anti-diffusive HLL scheme for the electronic M_1 model in the diffusion limit.

C. Chalons[1], S. Guisset[1]

Abstract: In this work, an asymptotic-preserving scheme is proposed for the electronic M_1 model in the diffusion limit. A very simple modification of the HLL numerical viscosity is considered in order to capture the correct asymptotic limit in the diffusion limit. This alteration also ensures the admissibility of the numerical solution under a suitable CFL condition. Interestingly, it is proved that the new scheme can also be understood as a Godunov-type scheme based on a suitable approximate Riemann solver. Various numerical test cases are performed and the results are compared with a standard HLL scheme and an explicit discretisation of the limit diffusion equation.

Key words: asymptotic-preserving scheme, diffusion limit, Godunov-type scheme, entropic angular M_1 model, plasma physics.

1 Introduction and governing equations

General introduction. Spitzer and Härm were the first to propose an electron transport theory in a fully ionised plasma without magnetic field [42]. They derived the electron plasma transport coefficients by solving the electron kinetic equation and using the expansion of the electron mean free path over the temperature scale length (denoted ε in this paper). For that, they assumed that the isotropic part of the electron distribution function remains close to the Maxwellian. In the case of non-local regimes [40], the Spitzer-Härm theory is not valid anymore. Considering for instance the case of inertial confinement fusion, the plasma particles may have an energy distribution which is far from the thermodynamic equilibrium so that the fluid description is not adapted. At the same time, a kinetic description is accurate to describe such processes but is also very expensive from the computational point of view and for most of real physical applications. Kinetic codes are indeed often limited to time and length scales much shorter than those studied with fluid simulations. Therefore, it is essential to be able to

[1]Laboratoire de Mathématiques de Versailles. Contact: sebastien.guisset@uvsq.fr

describe kinetic effects using reduced kinetic codes and operating on fluid time scales.

Entropic angular moments models can be seen as a compromise between kinetic and fluid models. On the one hand, they are less expensive than kinetic models since the number of variables is less. On the other hand, they provide more accurate results than fluid models. The main point in moments models is the definition of the closure relation which aims at giving the highest-order moment as a function of the lower-order ones. This closure relation corresponds to an approximation of the underlying distribution function. In [35, 38, 39, 43, 1], closures based on entropy minimisation principles are investigated. It has been shown that such a choice enables to recover fundamental properties such as the positivity of the underlying distribution function, the hyperbolicity of the model and an entropy dissipation property [24, 37, 35].

As we will see, the moments model under consideration here is based on an angular moments extraction. The kinetic equation is integrated with respect to the velocity direction only, while the velocity modulus is kept as a variable. The closure is based on an entropy minimisation principle and gives the angular M_1 model. This model is used in numerous applications such as radiative transfer [5, 44] or electron transport [36, 18, 26]. It satisfies fundamental properties and allows to recover an asymptotic diffusion equation in long time and small mean free path regimes [19], as will be seen hereafter.

In order to perform numerical simulations, the HLL scheme [29] is often used for the M_1 electronic model since it ensures the positivity of the first angular moment and the flux limitation property. However, this scheme does not degenerate correctly in the diffusive limit and necessitates extremely fine meshes to provide reasonable numerical approximations in this regime. In order to overcome this issue, the so-called asymptotic-preserving (AP) schemes in the sense of Jin-Levermore [31, 30] have been proposed over the last years to handle multi-scale situations, see for instance [10, 2, 20, 34, 8, 17, 32, 16, 15, 14] and the references therein. In particular, one of the most productive approach originated from Gosse-Toscani [23] is based on suitable modifications of approximate Riemann solvers in Godunov-type methods, see for instance [12, 11, 5, 13, 6].

Governing equations and numerical schemes. In the present work, we consider the M_1 model for the electronic transport [18, 28]. Ions are supposed to be fixed and electron-electron collisions are not considered. The angular moment model reads

$$
\begin{cases}
\partial_t f_0(t,x,\zeta) + \zeta\partial_x f_1(t,x,\zeta) + E(x)\partial_\zeta f_1(t,x,\zeta) = 0, \\
\partial_t f_1(t,x,\zeta) + \zeta\partial_x f_2(t,x,\zeta) + E(x)\partial_\zeta f_2(t,x,\zeta) \\
\qquad\qquad - \dfrac{E(x)}{\zeta}(f_0(t,x,\zeta) - f_2(t,x,\zeta)) = -\dfrac{2\alpha_{ei}(x) f_1(t,x,\zeta)}{\zeta^3},
\end{cases}
\tag{1}
$$

where f_0, f_1 and f_2 are the first three angular moments of the electron distribution function $f = f(t,x,\mu,\zeta)$, where t and x are the time and space variables, and μ and ζ represent the angle and the modulus of the velocity. Omitting the x and t dependency for the sake of clarity, they are given by

$$
\begin{gathered}
f_0(\zeta) = \zeta^2 \int_{-1}^{1} f(\mu,\zeta)d\mu, \quad f_1(\zeta) = \zeta^2 \int_{-1}^{1} f(\mu,\zeta)\mu d\mu, \\
f_2(\zeta) = \zeta^2 \int_{-1}^{-1} f(\mu,\zeta)\mu^2 d\mu.
\end{gathered}
\tag{2}
$$

In (1), the $\alpha_{ei} > 0$ positive function of x and $E = E(x)$ is the electrostatic field. In order to close this model, one has to define f_2 as a function of f_0 and f_1. Here, we consider that the closure relation originates from an entropy minimisation principle [35, 38] and that f_2 can be computed as a function of f_0 and f_1 as follows,

$$
f_2(t,x,\zeta) = \chi\Big(\frac{f_1(t,x,\zeta)}{f_0(t,x,\zeta)}\Big) f_0(t,x,\zeta), \quad \text{with} \quad \chi(\alpha) = \frac{1+\alpha^2+\alpha^4}{3}, \tag{3}
$$

see [18, 19]. The set of admissible states is defined by

$$
\mathcal{A} = \Big((f_0, f_1) \in \mathbb{R}^2, \; f_0 \geq 0, \; |f_1| \leq f_0\Big), \tag{4}
$$

which gives the existence of a nonnegative distribution function from the angular moments under consideration, see [41].

In [25, 27], a numerical scheme was proposed for the electronic M_1 model. It is based on the definition of an approximate Riemann solver, the intermediate states of which are chosen in order to obtain the asymptotic-preserving property. In the present work, the proposed procedure is different and follows the same approach as the one in [16]. More precisely, the asymptotic behavior of the usual HLL scheme is studied in the diffusive regime and the numerical viscosity is modified in order to capture the correct asymptotic limit. This modification is proposed in such a way that the admissibility of the numerical solution of the scheme holds true under suitable CFL conditions. Moreover, we will show that the new scheme can be understood by means of a suitable approximate Riemann solver. We also mention from now on that unlike [25, 27], the approach followed here allows to naturally recover the mixed derivatives arising in the diffusive limit.

Outline. The outline of the paper is as follows. We start by introducing the diffusive limit of the M_1 model in Section 2. In Section 3, we neglect the electric field by setting $E = 0$ and we study the HLL scheme is in the diffusive regime. Then, a very simple modification of the numerical viscosity is proposed and keeps the admissibility of the numerical solution. In Section 4, it is shown that the modified scheme can be understood as a Godunov-type scheme associated with a suitable approximate Riemann solver. In Section 5, the strategy is extended to the general model (1) with electric field. In Section 6, numerical examples are presented in different collisional regimes. Finally, conclusions and perspectives are given.

2 Diffusion limit

In this section, the diffusive limit of the electronic M_1 model (1) is introduced. For that, we consider a diffusive scaling and use a formal Hilbert expansion. More precisely, let us introduce the following diffusion scaling

$$\tilde{t} = t/t^*, \quad \tilde{x} = x/x^*, \quad \tilde{\zeta} = \zeta/v_{th}, \quad \tilde{E} = Ex^*/v_{th}^2$$

with the characteristic quantities t^* and x^* are chosen such that $\tau_{ei}/t^* = \varepsilon^2$, $\lambda_{ei}/x^* = \varepsilon$, where τ_{ei} is the electron-ion collisional period , λ_{ei} the electron-ion mean free path and v_{th} the thermal velocity defined by $v_{th} = \lambda_{ei}/\tau_{ei}$. The positive parameter ε is devoted to tend to zero. Rewriting (1) in dimensionless variables and removing the tildes from the new variables, the equations take the form

$$\begin{cases} \varepsilon\partial_t f_0(t,x,\zeta) + \zeta\partial_x f_1(t,x,\zeta) + E(x)\partial_\zeta f_1(t,x,\zeta) = 0, \\ \varepsilon\partial_t f_1(t,x,\zeta) + \zeta\partial_x f_2(t,x,\zeta) + E(x)\partial_\zeta f_2(t,x,\zeta) \\ \qquad\qquad - \dfrac{E(x)}{\zeta}(f_0(t,x,\zeta) - f_2(t,x,\zeta)) = -\dfrac{2\sigma(x)}{\zeta^3}\dfrac{f_1(t,x,\zeta)}{\varepsilon}, \end{cases} \tag{5}$$

where the coefficient σ is a non-negative function of x defined by

$$\sigma(x) = \frac{\tau_{ei}\alpha_{ei}(x)}{v_{th}^3}.$$

Introducing the following Hilbert expansion of f_0 and f_1

$$\begin{cases} f_0 = f_0^0 + \varepsilon f_0^1 + O(\varepsilon^2), \\ f_1 = f_1^0 + \varepsilon f_1^1 + O(\varepsilon^2), \end{cases} \tag{6}$$

the second equation of (5) taken at order ε^{-1} leads to

$$f_1^0 = 0. \tag{7}$$

Using the definition (3) of f_2, it follows that

$$f_2^0 = f_0^0/3. \tag{8}$$

Inserting again the Hilbert expansion (6) into the second equation of (5) gives now at order ε^0

$$f_1^1 = -\frac{\zeta^4}{6\sigma}\partial_x f_0^0 - \frac{E\zeta^3}{6\sigma}\partial_\zeta f_0^0 + \frac{E\zeta^2}{3\sigma} f_0^0. \tag{9}$$

Finally, using the previous equation into the first equation of (5) at order ε^1, the following limit equation is obtained

$$\begin{aligned}\partial_t f_0^0 + \zeta\partial_x\Big(- \frac{\zeta^4}{6\sigma}\partial_x f_0^0 - \frac{E\zeta^3}{6\sigma}\partial_\zeta f_0^0 + \frac{E\zeta^2}{3\sigma} f_0^0\Big) \\ + E\partial_\zeta\Big(- \frac{\zeta^4}{6\sigma}\partial_x f_0^0 - \frac{E\zeta^3}{6\sigma}\partial_\zeta f_0^0 + \frac{E\zeta^2}{3\sigma} f_0^0\Big) = 0.\end{aligned} \tag{10}$$

In the case $E = 0$ with no electric field, a classical diffusion equation with diffusion coefficient $-\zeta^5/6\sigma$ is recovered. In the general case, this limit equation involves mixed x and ζ derivatives leading to a non isotropic diffusion. Note also that the source term $E(f_0 - f_2)/\zeta$ brings its own contribution to the diffusive limit by adding the term $(E\zeta^2/(3\sigma))f_0^0$ in the right side of (9) and finally in the x and ζ derivatives of (10).

3 Derivation of an asymptotic-preserving scheme in the case with no electric field

In the case with no electric field, the electronic M_1 model reads

$$\begin{cases} \partial_t f_0(t,x,\zeta) + \zeta\partial_x f_1(t,x,\zeta) = 0, \\ \partial_t f_1(t,x,\zeta) + \zeta\partial_x f_2(t,x,\zeta) = -\dfrac{2\alpha_{ei}(x)}{\zeta^3} f_1(t,x,\zeta) \end{cases} \tag{11}$$

and the limit equation (10) writes

$$\partial_t f_0^0(t,x) - \zeta\partial_x\Big(\frac{\zeta^4}{6\sigma(x)}\partial_x f_0^0(t,x)\Big) = 0. \tag{12}$$

In this section, we present a numerical scheme which preserves the asymptotic behaviour (12).

We denote by Δx and Δt the space and time steps, respectively. We define the mesh interfaces $x_{j+1/2} = j\Delta x$ for $j \in \mathbb{Z}$ and the intermediate times $t^n = n\Delta t$ for $n \in \mathbb{N}$. We also define the mid-points $x_j = (x_{j-1/2} + x_{j+1/2})/2$ for $j \in \mathbb{Z}$. At each time t^n, f_{0i}^n and f_{1i}^n represent an approximation of the exact solutions f_0 and f_1 on the interval $[x_{j-1/2}, x_{j+1/2})$, $j \in \mathbb{Z}$, and we look for an approximation of the solutions at time t^{n+1}.
Note that in this section, ζ is a given constant value.

3.1 Limit of the classical HLL approach and simple modification

In this part, the limit behaviour of the classical HLL approach is presented and a very simple modification is proposed. In the present case, it is natural to use a mixed explicit-implicit treatment to deal with the stiff source term. More precisely, a classical HLL scheme with an implicit treatment of the source term is considered and it writes

$$\begin{cases} \dfrac{f_{0i}^{n+1}-f_{0i}^{n}}{\Delta t}+\dfrac{f_{1i+1/2}^{n}-f_{1i-1/2}^{n}}{\Delta x}=0, \\ \dfrac{f_{1i}^{n+1}-f_{1i}^{n}}{\Delta t}+\dfrac{f_{2i+1/2}^{n}-f_{2i-1/2}^{n}}{\Delta x}=-\dfrac{2\alpha_{ei}f_{1i}^{n+1}}{\zeta^{3}}, \end{cases} \tag{13}$$

where the numerical fluxes $f_{1,i+1/2}^{n}$ and $f_{2,i+1/2}^{n}$ write

$$\begin{cases} f_{1,i+1/2}^{n}=\dfrac{\zeta}{2}(f_{1i+1}^{n}+f_{1i}^{n})-\dfrac{a_x}{2}(f_{0i+1}^{n}-f_{0i}^{n}), \\ f_{2,i+1/2}^{n}=\dfrac{\zeta}{2}(f_{2i+1}^{n}+f_{2i}^{n})-\dfrac{a_x}{2}(f_{1i+1}^{n}-f_{1i}^{n}). \end{cases} \tag{14}$$

The wave speed a_x is fixed using the ideas introduced in [4]. More precisely, it is known from [35] that the electronic M_1 model without electric field (11) is hyperbolic symmetrizable and that the eigenvalues of the Jacobian matrix lies in the interval $[-\zeta,\zeta]$. Therefore, we set $a_x=\zeta$.

In order to perform the asymptotic analysis of the scheme, we consider the diffusive scaling and we introduce the following discrete Hilbert expansion of f_{0i}^{ε} and f_{1i}^{ε}, namely

$$\begin{cases} f_{0i}^{n,\varepsilon}=f_{0i}^{n,0}+\varepsilon f_{0i}^{n,1}+O(\varepsilon^2), \\ f_{1i}^{n,\varepsilon}=f_{1i}^{n,0}+\varepsilon f_{1i}^{n,1}+O(\varepsilon^2). \end{cases} \tag{15}$$

system (13) rewrites

$$\begin{cases} f_{0i}^{n+1}=f_{0i}^{n}-\dfrac{\Delta t}{\varepsilon\Delta x}(f_{1i+1/2}^{n}-f_{1i-1/2}^{n}), \\ f_{1i}^{n+1}=\dfrac{\varepsilon^2}{\varepsilon^2+\dfrac{2\sigma_i\Delta t}{\zeta^3}}\Big(f_{1i}^{n}-\dfrac{\Delta t}{\varepsilon\Delta x}(f_{2i+1/2}^{n}-f_{2i-1/2}^{n})\Big), \end{cases} \tag{16}$$

and the second equation of (16) gives at order $1/\varepsilon$

$$f_{1i}^{n+1,0}=0, \qquad \text{then} \qquad f_{2i}^{n+1,0}=f_{0i}^{n+1,0}/3 \ \text{ for all } n.$$

The same equation at the next order leads to

$$f_{1i}^{n+1,1}=-\frac{\zeta^4}{6\sigma_i}\frac{f_{0i+1}^{n,0}-f_{0i-1}^{n,0}}{2\Delta x} \ \text{ for all n,} \tag{17}$$

which is correctly consistent with (9) in the case with no electric field ($E = 0$). We thus clearly have by (14) that

$$f^n_{1,i+1/2} = \frac{\zeta}{2}(f^{n,1}_{1i+1} + f^{n,1}_{1i}) - \frac{a_x}{2}\frac{\Delta x}{\varepsilon}\frac{f^n_{0i+1} - f^n_{0i}}{\Delta x}.$$

We note that the centred part of this numerical flux is consistent with f_1^1 by (9) with $E = 0$ (thanks to (17)), but also that the diffusion term behaves like $O(\Delta x/\varepsilon)$. Therefore the numerical viscosity of the HLL scheme leads to a wrong asymptotic behavior in the diffusive regime at a given fixed mesh size Δx.

In order to overcome this major drawback and following [16, 15, 14], we propose to modify the numerical fluxes (14) such that

$$\begin{cases} f^n_{1,i+1/2} = \frac{\zeta}{2}(f^n_{1i+1} + f^n_{1i}) - \frac{a_x\theta_{i+1/2}}{2}(f^n_{0i+1} - f^n_{0i}), \\ f^n_{2,i+1/2} = \frac{\zeta}{2}(f^n_{2i+1} + f^n_{2i}) - \frac{a_x\theta_{i+1/2}}{2}(f^n_{1i+1} - f^n_{1i}), \end{cases} \tag{18}$$

where $\theta_{i+1/2}$ is a free parameter chosen in such a way that in the diffusive limit $\theta_{i+1/2} = O(\varepsilon)$. Therefore, we assume that in the diffusive regime $\theta_{i+1/2}$ can be written under the form

$$\theta = \varepsilon\theta^1 + O(\varepsilon^2).$$

With such a modification, the numerical viscosity of the HLL scheme behaves like $\mathcal{O}(\Delta x)$ in the diffusive regime and the first equation of (16) gives at order ε^0

$$\begin{aligned} &\frac{f^{n+1,0}_{0i} - f^{n,0}_{0i}}{\Delta t} - \zeta\frac{f^{n,1}_{1i+1} - f^{n,1}_{1i-1}}{2\Delta x} \\ &\qquad + a_x\frac{\theta^1_{i+1/2}f^{n,0}_{0i+1} - (\theta^1_{i+1/2} + \theta^1_{i-1/2})f^{n,0}_{0i} + \theta^1_{i-1/2}f^{n,0}_{0i-1}}{2\Delta x} = 0. \end{aligned} \tag{19}$$

By inserting (17) into (19) one obtains a numerical scheme which is now consistent with the limit equation (12).

Now, it remains to propose an explicit choice of θ which ensures the realisability requirement of the numerical solution under an uniform (with respect to ε) CFL condition on the time step Δt. This is the aim of the next section.

3.2 Admissibility requirement

In the previous part, we proposed a very simple modification of the HLL numerical fluxes that enables to capture the correct asymptotic limit. At this stage, it is natural to wonder how such a modification may affect the admissibility requirement (4) of the numerical solution since the numerical viscosity of the scheme has been reduced when ε tends to zero by the correction parameter θ. Given an admissible solution at a time t^n, we now give the conditions on θ and on the time step Δt to ensure the admissibility of the numerical solution at time t^{n+1}.

Theorem 1. *The modified scheme (13)-(18) preserves the admissibility of the numerical solution under the following conditions*

$$\Delta t \leq \frac{\Delta x}{a_x}, \quad \textit{and} \quad \theta_{i+1/2} = \max(\theta^1_{i+1/2}, \theta^2_{i+1/2}), \quad \forall\, i, \tag{20}$$

where

$$\theta^1_{i+1/2} = \max\Big(\frac{|f^n_{1i}|}{f^n_{0i}}, \frac{|f^n_{1i+1}|}{f^n_{0i+1}}\Big), \;\; \theta^2_{i+1/2} = \max\Big(\frac{|f^n_{1i} + \alpha_i f^n_{2i}|}{f^n_{0i} + \alpha_i f^n_{1i}}, \frac{|f^n_{1i+1} + \alpha_{i+1} f^n_{2i+1}|}{f^n_{0i+1} + \alpha_{i+1} f^n_{1i+1}}\Big),$$

and

$$\alpha_i = \frac{1}{1 + \dfrac{2\sigma_i \Delta t}{\zeta^3}}. \tag{21}$$

Proof. Let us first prove that $f^{n+1}_{0i} \geq 0$ for all $i \in \mathbb{N}$.
Using (18), the first equation of (13) rewrites

$$\begin{aligned} f^{n+1}_{0i} = f^n_{0i}(1 - \frac{\zeta \Delta t(\theta_{i+1/2} + \theta_{i-1/2})}{2\Delta x}) &+ \frac{\zeta \Delta t}{2\Delta x}(\theta_{i+1/2} f^n_{0i+1} - f^n_{1i+1}) \\ &+ \frac{\zeta \Delta t}{2\Delta x}(\theta_{i-1/2} f^n_{0i-1} + f^n_{1i-1}). \end{aligned}$$

In order to ensure the positivity of f^{n+1}_{0i}, it is sufficient to prove that the three terms in the right-hand side are positive. One obtains the positivity of f^{n+1}_{0i} under the conditions

$$\Delta t \leq \frac{2\Delta x}{a_x(\theta_{i+1/2} + \theta_{i-1/2})} \quad \text{and} \quad \theta_{i+1/2} = \max(\frac{|f^n_{1i}|}{f^n_{0i}}, \frac{|f^n_{1i+1}|}{f^n_{0i+1}}), \quad \forall\, i, \tag{22}$$

Let us now prove that $|f^{n+1}_{1i}| \leq f^{n+1}_{0i}$ for all $i \in \mathbb{N}$ which is equivalent to $f^{n+1}_{0i} + f^{n+1}_{1i} \geq 0$ and $f^{n+1}_{0i} - f^{n+1}_{1i} \geq 0$. We will focus on $f^{n+1}_{0i} + f^{n+1}_{1i} \geq 0$, the treatment of the other inequality being similar. Considering (13) leads to

$$\begin{aligned} f^{n+1}_{0i} + f^{n+1}_{1i} =& \frac{\zeta \Delta t}{2\Delta x}\Big(\theta_{i+1/2} f^n_{0i+1} - f^n_{1i+1} - \alpha f^n_{2i+1} + \alpha_i \theta_{i+1/2} f^n_{1i+1}\Big) \\ &+ \frac{\zeta \Delta t}{2\Delta x}\Big[\theta_{i-1/2} f^n_{0i-1} + f^n_{1i-1} + \alpha_i f^n_{2i-1} + \alpha_i \theta_{i-1/2} f^n_{1i-1}\Big] \\ + f^n_{0i} + \alpha_i f^n_{1i} &- \frac{\zeta \Delta t(\theta_{i+1/2} + \theta_{i-1/2})}{2\Delta x} f^n_{0i} - \frac{\zeta \Delta t \alpha_i(\theta_{i+1/2} + \theta_{i-1/2})}{2\Delta x} f^n_{1i}. \end{aligned}$$

It is sufficient to show that the three terms of the right-hand side are positive. The positivity of the first two terms is ensured provided that

$$\theta_{i+1/2} = \max\left(\frac{|f_{1i}^n + \alpha_i f_{2i}^n|}{f_{0i}^n + \alpha_i f_{1i}^n}, \frac{|f_{1i+1}^n + \alpha_{i+1} f_{2i+1}^n|}{f_{0i+1}^n + \alpha_{i+1} f_{1i+1}^n}\right). \tag{23}$$

The positivity of the third term is ensured as soon as

$$\Delta t \leq \frac{2\Delta x}{a_x(\theta_{i+1/2} + \theta_{i-1/2})},$$

which is the same CFL condition as for the first admissiblity condition $f_0^{n+1} \geq 0$ for all i. The same approach but now considering $f_{0i}^{n+1} - f_{1i}^{n+1}$ gives the same conditions. □

Remark 1. *It is interesting to notice that in the diffusive regime, $\theta_{i+1/2}$ defined by (22)-(23) as well as f_{1i}^n $\forall i \in \mathbb{N}$ behave like $O(\varepsilon)$ in ε. Indeed using the diffusive scaling and a direct development in ε in the second equation of (16) gives*

$$f_{1i}^{n+1} = -\varepsilon \frac{\zeta^4}{6\sigma_i} \frac{f_{0i+1}^{n,0} - f_{0i-1}^{n,0}}{2\Delta x} + O(\varepsilon^2). \tag{24}$$

Remark 2. *Observe that the quantity $(f_1 + \alpha f_2)/(f_0 + \alpha f_1)$ remains smaller or equal to 1. Indeed, by introducing the anisotropic parameter x defined such that*

$$x = f_1/f_0,$$

and using the definition (3) we get

$$\frac{f_1 + \alpha f_2}{f_0 + \alpha f_1} = \frac{x + \alpha\chi(x)}{1 + \alpha x},$$

which remains smaller or equal to 1 for all $\alpha \in [0, 1]$ and $x \in [-1, 1]$. This quantity is displayed in terms of α and x on Figure 1.

Remark 3. *It is not really possible to use the CFL condition (22) as it stands since the parameter θ depends on α which depends itself on Δt by* (21). *In order to overcome this issue, we use the fact that θ is equal or smaller than 1 and we consider the CFL condition*

$$\Delta t \leq \frac{\Delta x}{a_x}.$$

Therefore, at each time step, we start computing Δt independently of θ by using (20), then we obtain α and θ with (21) *and* (20). *Finally, the quantities can be updated at the next time step with the scheme (13) and (18).*

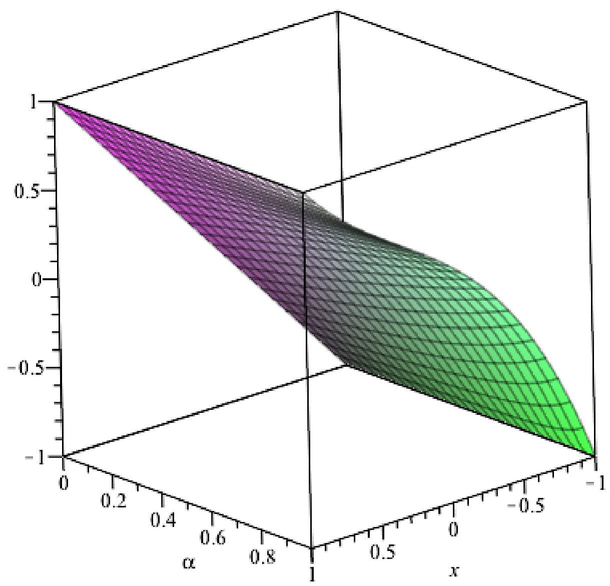

Figure 1: Representation of the quantity $(1+\alpha\chi(x))/(1+\alpha x)$ in terms of α and x.

4 Approximate Riemann solvers interpretation

In this part we show that the numerical scheme derived in the previous section is equivalent to a Godunov-type scheme based on a particular approximate Riemann solver.

Extending the ideas introduced in [22, 21, 9, 15], we consider an approximate solver of the following form

$$U_{\mathcal{R}}(x/t, U^L, U^R) = \begin{cases} U^L(t) & \text{if} \quad x/t < -a_x\theta, \\ U^{L*}(t) & \text{if} \quad -a_x\theta < x/t < 0, \\ U^{R*}(t) & \text{if} \quad 0 < x/t < a_x\theta, \\ U^R(t) & \text{if} \quad a_x < x/t, \end{cases} \tag{25}$$

where the intermediate states $U^{L*}(t) = {}^t(f_0^{L*}, f_1^{L*}(t))$, $U^{R*}(t) = {}^t(f_0^{R*}, f_1^{R*}(t))$, the minimum and maximum speeds of propagation $-a_x$ and a_x and the states $U^L(t)$ and $U^R(t)$ have to be defined. We note that the proposed approximate Riemann solver is made of three well-ordered waves, the second one being stationary. The quantities $U^L(t)$ and $U^R(t)$ stand for $U^L(t) = {}^t(f_0^L, f_1^L(t))$ and $U^R(t) = {}^t(f_0^R, f_1^R(t))$. At this stage, it is crucial to notice that the second component of the constant (in space) states U^L, U^{L*}, U^{R*}, U^R

actually depend on t and that we will have $f_1^L(0) = f_1^L$ and $f_1^R(0) = f_1^R$. The structure of the approximate Riemann solver is displayed on Fig. 2.

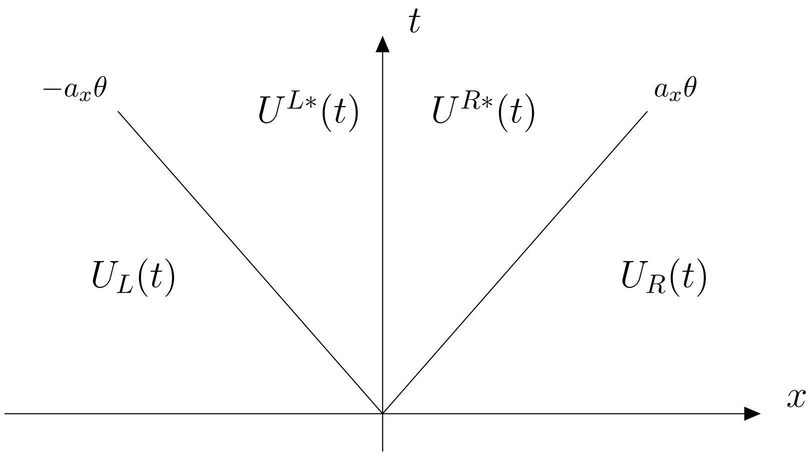

Figure 2: Structure of the approximate Riemann solver.

Following the classical Godunov-type procedure to compute a piecewise constant approximate solution U_i^{n+1} on each cell $\mathcal{D}_i =]x_{i-1/2}, x_{i+1/2}[$ at time t^{n+1}, the exact solution w of (11) is averaged on each cell and

$$U_i^{n+1} \approx \frac{1}{\Delta x} \int_{x_{i-1/2}}^{x_{i+1/2}} w(\Delta t, x) dx. \tag{26}$$

Instead of solving (11) exactly, one suggests to use the approximate Riemann solver (25) at each interface and to replace w by $\tilde{w}$ defined as the juxtaposition of the approximate Riemann solutions as follows

$$\tilde{w}(x,t) = U_{\mathcal{R}}((x - x_{i+1/2})/t, U_i^n, U_{i+1}^n), \text{ if } x \in [x_i, x_{i+1}].$$

Let us now explain the derivation of the intermediate states $U^{L*}(t)$ and $U^{R*}(t)$. Following [29], we impose that the integral at time Δt of the approximate Riemann solution (25) over the slab $[-\frac{\Delta x}{2}, \frac{\Delta x}{2}]$ under the CFL condition $\Delta t \leq \dfrac{\Delta x}{2a_x\theta}$ equals the integral of the exact Riemann solution to (11), which gives here for the first equation

$$\begin{aligned}(\frac{\Delta x}{2} - a_x\theta\Delta t) f_0^L + a_x\theta\Delta t f_0^{L*} + a_x\theta\Delta t f_0^{R*} + (\frac{\Delta x}{2} - a_x\theta\Delta t) f_0^R& \\ = \frac{\Delta x}{2}(f_0^L + f_0^R) - \zeta \int_0^{\Delta t} (f_1^R(t) - f_1^L(t)) dt&\end{aligned}$$

that is to say

$$\frac{f_0^{L*}+f_0^{R*}}{2}=\frac{f_0^L+f_0^R}{2}-\frac{\zeta}{2a_x\theta\Delta t}\int_0^{\Delta t}(f_1^R(t)-f_1^L(t))dt,$$

which can be approximated by

$$\frac{f_0^{L*}+f_0^{R*}}{2}=\frac{f_0^L+f_0^R}{2}-\frac{\zeta}{2a_x\theta}(f_1^R-f_1^L),$$

using the left rectangle (time explicit) quadrature formula and since $f_1^R(0)=f_1^R$ and $f_1^L(0)=f_1^L$. Therefore a natural choice consists in setting

$$f_0^{L*}=f_0^{R*}=\frac{f_0^L+f_0^R}{2}-\frac{\zeta}{2a_x\theta}(f_1^R-f_1^L). \tag{27}$$

Before considering the second equation of (11), let us define $f_1^R(t)$ and $f_1^L(t)$ in the approximate Riemann solver (25). Since there is a source term, using the ideas of [3], we compute $f_{1i}(t)$ as solution of the following ordinary differential equation

$$\frac{df_1(t)}{dt}=-\frac{2\alpha_{ei}f_1(t)}{\zeta^3}, \tag{28}$$

with $f_1(0)=f_1^L$ or $f_1(0)=f_1^R$. This equation can be solved exactly, however, in order to recover the numerical scheme (13)-(18), we choose a standard implicit discretisation which gives

$$f_1^{L,R}(t)=\frac{1}{1+\dfrac{2\sigma_{L,R}\Delta t}{\zeta^3}}f_1^{L,R}, \quad \forall t\in[0,\Delta t]. \tag{29}$$

Considering now the second equation of (11), the same approach gives

$$\begin{aligned}(\frac{\Delta x}{2}-a_x\theta\Delta t)f_1^L(\Delta t)+a_x\theta\Delta t f_1^{L*}(\Delta t)+a_x\theta\Delta t f_1^{R*}(\Delta t)+(\frac{\Delta x}{2}-a_x\theta\Delta t)f_1^R(\Delta t)\\ =\frac{\Delta x}{2}(f_1^L(0)+f_1^R(0))-\zeta\int_0^{\Delta t}(f_2^R(t)-f_2^L(t))dt-\int_0^{\Delta t}\int_{-\frac{\Delta x}{2}}^{\frac{\Delta x}{2}}\frac{2\alpha_{ei}(x)}{\zeta^3}f_1dxdt,\end{aligned}$$

that is to say, since $f_1^R(0)=f_1^R$ and $f_1^L(0)=f_1^L$,

$$\begin{aligned}\frac{f_1^{L*}(\Delta t)+f_1^{R*}(\Delta t)}{2}&=\frac{f_1^L(\Delta t)+f_1^R(\Delta t)}{2}+\frac{\Delta x}{4a_x\theta\Delta t}(f_1^L+f_1^R)\\ &-\frac{\Delta x}{4a_x\theta\Delta t}(f_1^L(\Delta t)+f_1^R(\Delta t))-\frac{\zeta}{2a_x\theta\Delta t}\int_0^{\Delta t}(f_2^R(t)-f_2^L(t))dt\\ &-\frac{1}{2a_x\theta\Delta t}\int_0^{\Delta t}\int_{-\frac{\Delta x}{2}}^{\frac{\Delta x}{2}}\frac{2\alpha_{ei}(x)}{\zeta^3}f_1dxdt.\end{aligned} \tag{30}$$

Let us try to simplify this equality. We first notice that

$$\int_0^{\Delta t}\int_{-\frac{\Delta x}{2}}^{\frac{\Delta x}{2}} \frac{2\alpha_{ei}(x)}{\zeta^3} f_1 dx dt = \int_0^{\Delta t}\int_{-a_x\theta\Delta t}^{a_x\theta\Delta t} \frac{2\alpha_{ei}(x)}{\zeta^3} f_1 dx dt$$
$$+ (\frac{\Delta x}{2} - a_x\theta\Delta t)\int_0^{\Delta t} \frac{2\alpha_{ei}(x)}{\zeta^3} f_1 dx dt + (\frac{\Delta x}{2} - a_x\theta\Delta t)\int_0^{\Delta t} \frac{2\alpha_{ei}(x)}{\zeta^3} f_1 dx dt,$$

which gives by (28) to evaluate the last two integrals

$$\begin{aligned}\int_0^{\Delta t}\int_{-\frac{\Delta x}{2}}^{\frac{\Delta x}{2}} \frac{2\alpha_{ei}(x)}{\zeta^3} f_1 dx dt \approx &- (\frac{\Delta x}{2} - a_x\theta\Delta t)(f_1^R(\Delta t) - f_1^R) \\ &- (\frac{\Delta x}{2} - a_x\theta\Delta t)(f_1^L(\Delta t) - f_1^L) \\ &+ \int_0^{\Delta t}\int_{-a_x\theta\Delta t}^{a_x\theta\Delta t} \frac{2\alpha_{ei}(x)}{\zeta^3} f_1 dx dt.\end{aligned}$$

Now using a right-rectangle (time implicit) quadrature formula, we get

$$\begin{aligned}-\int_0^{\Delta t}\int_{-\frac{\Delta x}{2}}^{\frac{\Delta x}{2}} \frac{2\alpha_{ei}(x)}{\zeta^3} f_1 dx dt \approx &(\frac{\Delta x}{2} - a_x\theta\Delta t)(f_1^R(\Delta t) - f_1^R) \\ &+(\frac{\Delta x}{2} - a_x\theta\Delta t)(f_1^L(\Delta t) - f_1^L) \\ &-\frac{2a_x\theta\Delta t^2\alpha_{ei}^L}{\zeta^3} f_1^{L*}(\Delta t) - \frac{2a_x\theta\Delta t^2\alpha_{ei}^R}{\zeta^3} f_1^{R*}(\Delta t).\end{aligned} \tag{31}$$

Let us then use a left rectangle (time explicit) quadrature formula to write

$$\frac{\zeta}{2a_x\theta\Delta t}\int_0^{\Delta t}(f_2^R(t) - f_2^L(t))dt \approx \frac{\zeta}{2a_x\theta}(f_2^R - f_2^L). \tag{32}$$

Inserting (31) and (32) in (30) gives after easy calculation

$$\frac{f_1^{L*}(\Delta t) + f_1^{R*}(\Delta t)}{2} = \frac{f_1^L + f_1^R}{2} - \frac{\zeta}{2a_x\theta}(f_2^R - f_2^L) - \frac{\Delta t}{2}(\frac{2\alpha_{ei}^L}{\zeta^3} f_1^{L*}(\Delta t) + \frac{2\alpha_{ei}^R}{\zeta^3} f_1^{R*}(\Delta t)).$$

Following the same procedure as for the first equation we consider the intermediate states

$$\begin{cases} f_1^{L*}(\Delta t) = (\dfrac{1}{1 + \frac{2\Delta t\alpha_{ei}^L}{\zeta^3}})(\dfrac{f_1^L + f_1^R}{2} - \dfrac{\zeta}{2a_x\theta}(f_2^R - f_2^L)), \\ f_1^{R*}(\Delta t) = (\dfrac{1}{1 + \frac{2\Delta t\alpha_{ei}^R}{\zeta^3}})(\dfrac{f_1^L + f_1^R}{2} - \dfrac{\zeta}{2a_x\theta}(f_2^R - f_2^L)). \end{cases} \tag{33}$$

Now using the relation (26) but with the approximate Riemann solver instead of the exact one, and considering that θ takes a positive value $\theta_{i+1/2}$ at each interface, the numerical solution at time t^{n+1} is given by

$$
\begin{cases}
f_{0i}^{n+1} = \dfrac{a_x\theta_{i-1/2}\Delta t}{\Delta x} f^{R*}_{0i-1/2} & + (1 - \dfrac{a_x(\theta_{i-1/2}+\theta_{i+1/2})\Delta t}{\Delta x}) f^n_{0i} \\
& + \dfrac{a_x\theta_{i+1/2}\Delta t}{\Delta x} f^{L*}_{0i+1/2}, \\
f_{1i}^{n+1} = \dfrac{a_x\theta_{i-1/2}\Delta t}{\Delta x} f^{R*}_{1i-1/2}(\Delta t) & + (1 - \dfrac{a_x(\theta_{i-1/2}+\theta_{i+1/2})\Delta t}{\Delta x}) f_{1i}(\Delta t) \\
& + \dfrac{a_x\theta^{\Delta}_{i+1/2}t}{\Delta x} f^{L*}_{1i+1/2}(\Delta t).
\end{cases}
\tag{34}
$$

A direct calculation using the definitions (27)-(33)-(29) enables us to recover the scheme (13) with the numerical fluxes (18). Therefore the asymptotic-preserving scheme (13)-(18) can be interpretated as a Godunov-type scheme based on the approximate Riemann solver (25).

Conditions (20) on the parameter θ can be recovered by considering the intermediate states of (25). Indeed, since the numerical scheme (34) writes as a convex combinaison and the admissible set is convex, the admissibility of the intermediate states U^{L*} and U^{R*} yields the admissibility of the numerical solution at time t^{n+1} under the usual CFL condition

$$\Delta t \leq \frac{\Delta x}{2a_x||\theta||_\infty}.$$

Computing $f_0^{L*} \pm f_1^{L*}$ and $f_0^{R*} \pm f_1^{R*}$ and using the definitions (27) and (33) enables to recover the conditions (20) by a simple calculation.

5 Extension to the general model

In this part, we extend the asymptotic-preserving scheme we derived in the previous section to the M_1 model (1) with non zero electric field E.

5.1 General scheme

Extending our previous ideas, we use a j index to deal with the ζ variable and we propose the following numerical scheme

$$
\begin{aligned}
&\frac{f^{n+1}_{0ij} - f^n_{0ij}}{\Delta t} + \frac{f^n_{1i+1/2j} - f^n_{1i-1/2j}}{\Delta x} + \frac{f^n_{1ij+1/2} - f^n_{1ij-1/2}}{\Delta \zeta} = 0, \\
&\frac{f^{n+1}_{1ij} - f^n_{1ij}}{\Delta t} + \frac{f^n_{2i+1/2j} - f^n_{2i-1/2j}}{\Delta x} + \frac{f^n_{2ij+1/2} - f^n_{2ij-1/2}}{\Delta \zeta} \\
&\qquad - E_i \frac{(f^n_{0ij} - f^n_{2ij})}{\zeta_j} = -\frac{2\alpha_{ei,i} f^{n+1}_{1ij}}{\zeta_j^3},
\end{aligned}
\tag{35}
$$

where the numerical fluxes used are defined by

$$\begin{cases} f^n_{1,i+1/2j} = \dfrac{\zeta_j}{2}(f^n_{1i+1j} + f^n_{1ij}) - \dfrac{a_x\theta_{1i+1/2j}}{2}(f^n_{0i+1j} - f^n_{0ij}), \\ f^n_{2,i+1/2j} = \dfrac{\zeta_j}{2}(f^n_{2i+1j} + f^n_{2ij}) - \dfrac{a_x\theta_{1i+1/2j}}{2}(f^n_{1i+1j} - f^n_{1ij}), \end{cases} \tag{36}$$

and

$$\begin{cases} f^n_{1,ij+1/2} = \dfrac{E_i}{2}(f^n_{1ij+1} + f^n_{1ij}) - \dfrac{a_\zeta\theta_{2ij+1/2}}{2}(f^n_{0ij+1} - f^n_{0ij}), \\ f^n_{2,ij+1/2} = \dfrac{E_i}{2}(f^n_{2ij+1} + f^n_{2ij}) - \dfrac{a_\zeta\theta_{2ij+1/2}}{2}(f^n_{1ij+1} - f^n_{1ij}). \end{cases} \tag{37}$$

The correction coefficients θ_1 and θ_2 are fixed in order to ensure the admissibility requirement and the asymptotic-preserving property. We take $a_x = \zeta_j$ and $a_\zeta = |E_i|$. For the sake of clarity, we omit the dependency of the speed a_x in velocity modulus and a_ζ in space.

5.2 Properties

In this part, the properties of the numerical scheme (35)-(36)-(37) are detailed. It is first shown that the scheme preserves the admissibility of the numerical solution under suitable conditions, and then that the asymptotic-preserving property holds true.

Theorem 2. *The numerical scheme (35)-(36)-(37) preserves the set of admissible states $\mathcal{A}$ under the following conditions*

$$\Delta t \leq \min\Big(\frac{\Delta x\Delta\zeta}{a_x\Delta x + a_\zeta\Delta\zeta}, \frac{\Delta x\Delta\zeta}{a_x\Delta x + a_\zeta\Delta\zeta + 4||E||_\infty\Delta x}\Big), \tag{38}$$

and

$$\theta_{1i+1/2j} = \max(\theta^1_{1i+1/2j}, \theta^2_{1i+1/2j}), \quad \theta_{2ij+1/2} = \max(\theta^1_{2ij+1/2}, \theta^2_{2ij+1/2}), \tag{39}$$

with

$$\begin{aligned} \theta^1_{1i+1/2j} &= \max\Big(\frac{|f^n_{1ij}|}{f^n_{0ij}}, \frac{|f^n_{1i+1j}|}{f^n_{0i+1j}}\Big), \\ \theta^2_{1i+1/2j} &= \max\Big(\frac{|f^n_{1ij} + \alpha_{ij}f^n_{2ij}|}{f^n_{0ij} + \alpha_{ij}f^n_{1ij}}, \frac{|f^n_{1i+1j} + \alpha_{i+1j}f^n_{2i+1j}|}{f^n_{0i+1j} + \alpha_{i+1j}f^n_{1i+1j}}\Big), \\ \theta^1_{2ij+1/2} &= \max\Big(\frac{|f^n_{1ij}|}{f^n_{0ij}}, \frac{|f^n_{1ij+1}|}{f^n_{0ij+1}}\Big), \\ \theta^2_{2ij+1/2} &= \max\Big(\frac{|f^n_{1ij} + \alpha_{ij}f^n_{2ij}|}{f^n_{0ij} + \alpha_{ij}f^n_{1ij}}, \frac{|f^n_{1ij+1} + \alpha_{ij+1}f^n_{2ij+1}|}{f^n_{0ij+1} + \alpha_{ij+1}f^n_{1ij+1}}\Big). \end{aligned}$$

Proof. The proof follows exactly the same lines as in the case with no electric field. The property is obtained by direct computations of $f_{0ij}^{n+1} \pm f_{1ij}^{n+1}$ under the CFL condition

$$\Delta t \leq \min\Big(\frac{\Delta x \Delta\zeta}{a_x||\theta_1||\Delta x + a_\zeta||\theta_2||\Delta\zeta}, \qquad (40)$$

$$\frac{\Delta x \Delta\zeta}{a_x||\theta_1||\Delta x + a_\zeta||\theta_2||\Delta\zeta + ||\frac{\alpha E}{\zeta}(\frac{f_0^n - f_2^n}{f_0^n + \alpha f_1^n})||_\infty \Delta x \Delta\zeta}\Big).$$

□

Remark 4. *Introducing the anisotropic parameter x defined by $x = f1/f0$ and using the definition (3), we get*

$$\frac{f_0 - f_2}{f_0 + \alpha f_1} = \frac{1 - \chi(x)}{1 + \alpha x}.$$

This quantity is displayed in terms of α and x on Figure 3 and it is interesting to note that it is less than 2, which also applies to $(f_0^n - f_2^n)/(f_0^n + \alpha f_1^n)$ for all n. Therefore following the same procedure as in the case without electric field, instead of using (40), we consider the CFL condition (38) which is independent of θ.

The asymptotic-preserving property of the scheme is now stated.

Theorem 3. *(Consistency with the limit diffusion equation)*
In the limit ε tends to zero, the limit of the numerical scheme (35) is consistent with the limit diffusion equation (10).

Proof. Using again discrete Hilbert expansions the second equation of (35) at order $1/\varepsilon$ gives $f_{1ij}^{n+1,0} = 0$ and then $f_{2ij}^{n+1,0} = f_{0ij}^{n+1,0}/3$ for all n and j. The same equation at the next order leads to

$$f_{1ij}^{n+1,1} = -\frac{\zeta_j^3}{2\sigma_i}\Big(-\frac{\zeta_j}{3}\frac{f_{0i+1j}^{n,0} - f_{0i-1j}^{n,0}}{2\Delta x} + \frac{E_i}{3}\frac{f_{0ij+1}^{n,0} - f_{0ij-1}^{n,0}}{2\Delta\zeta} + \frac{2E_i}{3}\frac{f_{0ij}^{n,0}}{\zeta_j}\Big), \quad (41)$$

which is consistent with (9). Thanks to the correction parameters θ_1^ε and θ_2^ε, the numerical viscosity of the scheme behaves like $O(\Delta x)$ and the first

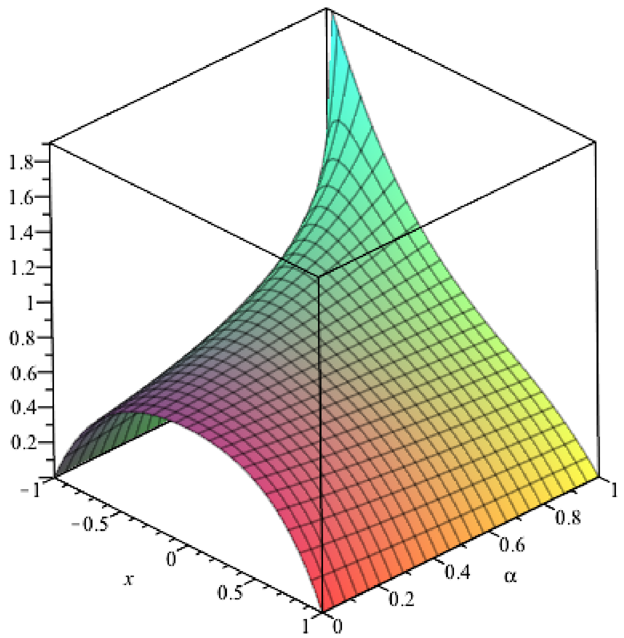

Figure 3: Representation of the quantity $(1-\chi(x))/(1+\alpha x)$ in terms of α and x.

equation of (35) gives at the order $O(\varepsilon^0)$

$$\begin{aligned}
&\frac{f_{0ij}^{n+1,0}-f_{0ij}^{n,0}}{\Delta t}-\zeta_j\frac{f_{1i+1j}^{n,1}-f_{1i-1j}^{n,1}}{2\Delta x}\\
&\qquad+a_x\frac{\theta_{1i+1/2j}^{1}f_{0i+1j}^{n,0}-(\theta_{1i+1/2j}^{1}+\theta_{1i-1/2j}^{1})f_{0ij}^{n,0}+\theta_{1i-1/2j}^{1}f_{0i-1j}^{n,0}}{2\Delta x}\\
&\qquad\quad-E_i\frac{f_{1ij+1}^{n,1}-f_{1ij-1}^{n,1}}{2\Delta\zeta}\\
&\qquad+a_\zeta\frac{\theta_{2ij+1/2}f_{0ij+1}^{n,0}-(\theta_{2ij+1/2}+\theta_{2ij-1/2})f_{0ij}^{n,0}+\theta_{2ij-1/2}f_{0ij-1}^{n,0}}{2\Delta\zeta}=0,
\end{aligned}\tag{42}$$

which is clearly consistent with the limit diffusion equation (10). □

5.3 Accuracy enhancement

In order to prepare the next section devoted to the numerical experiments, we briefly mention that a second-order type improvement of our scheme will be considered. The underlying strategy, based on the usual second-order Van

Leer's slope limiter [33] method, will lead to a significant improvement of the numerical solutions. More precisely and following [33], piecewise linear reconstructions are considered and the corresponding extrapolated values at each interface are used in the numerical fluxes (36)-(37). On the other hand, the θ_1 and θ_2 coefficients are still defined by (39). To conclude, the rigorous analysis (admissibility, asymptotic-preserving property...) of the proposed second-order type extension is not easy, see for instance [7], and it is postponed to a forthcoming study.

Remark 5. *In practice, the admissibility is checked at each time step. In case the numerical solution is not admissible, it is recomputed using the classical scheme with no reconstruction, in the spirit of the MOOD approach (see for instance [7] and the references therein).*

6 Numerical results

This section is devoted to numerical experiments. Depending on the collisional regime, our asymptotic-preserving scheme is compared to an explicit discretisation of the limit diffusion equation and with a standard HLL scheme.

Test 1 : relaxation of a gaussian profile in different collisional regimes.
In this first test case, three different collisional regimes are considered with the same initial condition given by

$$\begin{cases} f_0(t=0,x,\zeta) = \zeta^2 \exp(-(\zeta-2)^2) \exp(-x^2), \\ f_1(t=0,x,\zeta) = 0, \end{cases}$$

for (x,ζ) in $[-10:10] \times [0,6]$ and displayed on Fig. 4. The electric field E is taken to be constant and equal to 1. Neumann boundary conditions are considered and ghost cells are used from a practical point of view. The space step Δx equals $2.5 \cdot 10^{-2}$ and the modulus energy step $\Delta\zeta$ is $5 \cdot 10^{-2}$.

Test 1a : the free transport regime.
In this case, the collisional parameter α_{ei} is set to zero. On Fig. 5, we present the solutions obtained with the classical HLL scheme and our asymptotic-preserving scheme, with and without piecewise linear reconstruction. In this transport regime, one can observe that both schemes give the same results and that the piecewise linear reconstruction allows to reduce the numerical diffusion.

Test 1b : the diffusive regime.
In this case, the collisional parameter is set to 10^4. Fig 6 shows the f_0 profile obtained with the asymptotic-preserving scheme, the usual HLL scheme

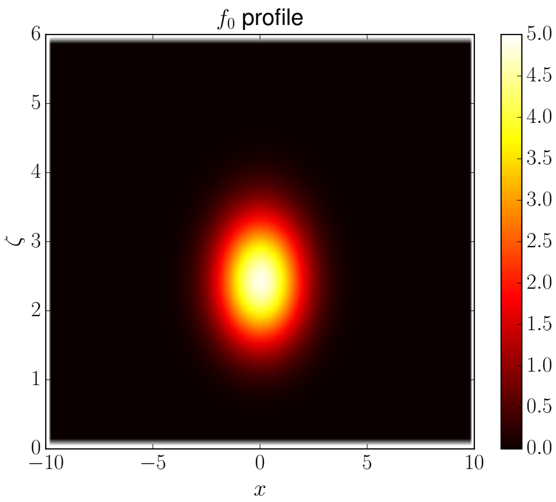

Figure 4: Representation of the f_0 profile at the initial time.

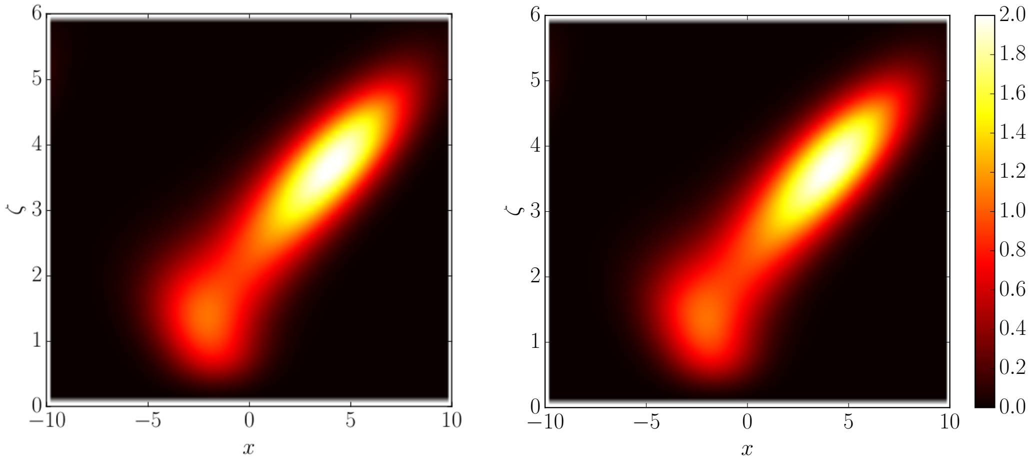

Figure 5: Test 1a : representation of the f_0 profiles obtained with a HLL scheme (right) and the AP scheme (left) at time $t = 2$ in the case without collisions.

and an explicit discretisation of the diffusion equation at times $t = 20$ and $t = 100$. The results given with the second-order extension are given on Fig 7. We clearly see that the classical HLL scheme is very diffusive while the asymptotic-preserving scheme gives a much more accurate numerical solution. However, at time $t = 100$, the solution is quite different from the expected diffusion profile. Turning now to the second-order extension, the asymptotic-preserving solution is now very close to the exact one, while the HLL scheme remains very diffusive.

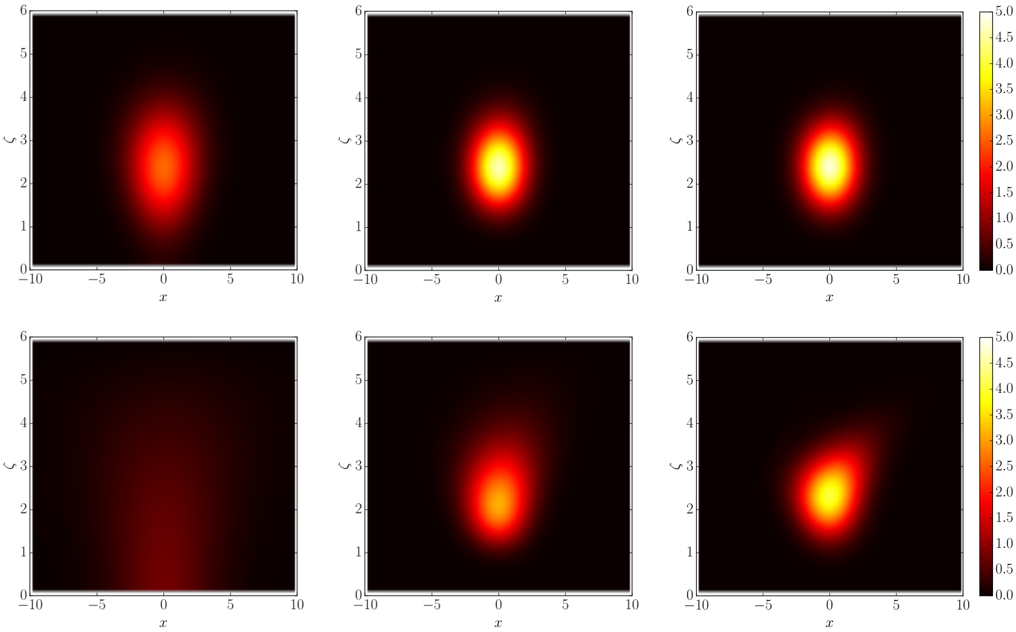

Figure 6: Test 1b : representation of the f_0 profiles obtained with the first order HLL scheme (left), the first order AP scheme (middle) and the diffusion scheme (right) at time $t = 20$ (top) and $t = 100$ (bottom) in the diffusive regime with $\alpha_{ei} = 10^4$.

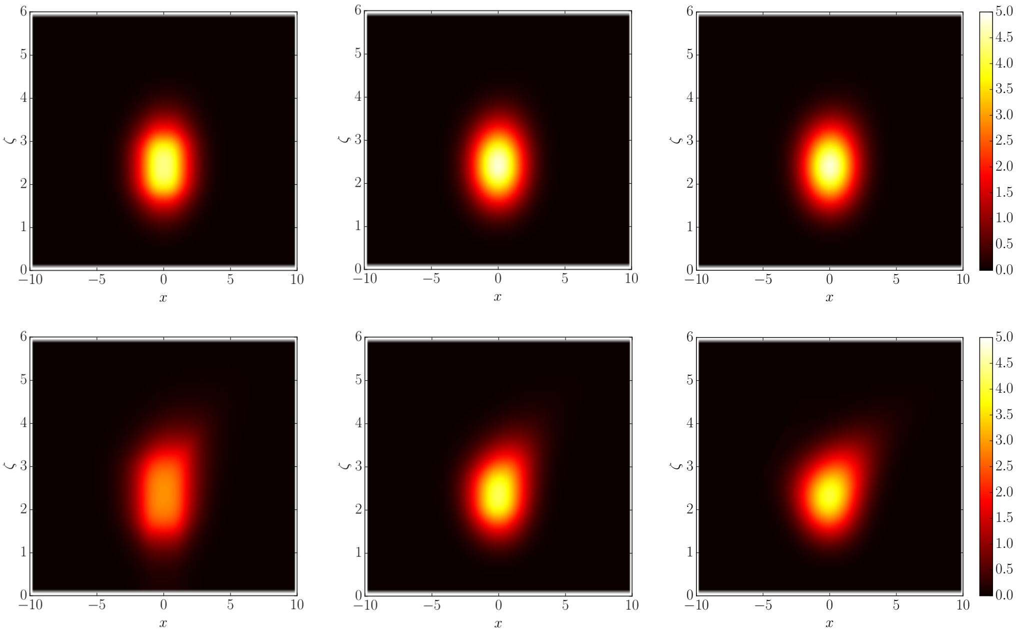

Figure 7: Test 1b : representation of the f_0 profiles obtained with the second order HLL scheme (left), the second order AP scheme (middle) and the diffusion scheme (right) at time $t = 20$ (top) and $t = 100$ (bottom) in the diffusive regime with $\alpha_{ei} = 10^4$.

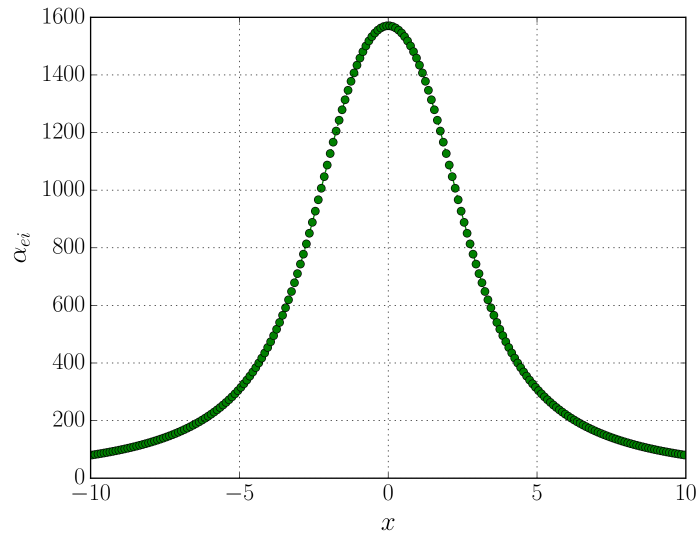

Figure 8: Test 1c : representation of the collisional parameter profile α_{ei}.

Test 1c : non-constant collisional parameter.
In this case, the collisional parameter α_{ei} depends on x and is given by

$$\alpha_{ei}(x) = 10^3 \cdot (\arctan(1 + 0.5 \cdot x) + \arctan(1 - 0.5 \cdot x),$$

see Fig. 8. On Fig. 9, one clearly sees that the solution obtained with the second-order HLL scheme is much more diffused than the one obtained with the second-order asymptotic-preserving scheme.

Test 2: Discontinuous f_0 profile with non constant electric field and non constant collision parameter.
We now consider the temporal evolution of a discontinuous f_0 profile with inhomogeneous electric field and non-constant collision parameter. The initial condition is discontinuous and writes

$$\begin{cases} f_0^{ini}(x,\zeta) = \begin{cases} \dfrac{4}{\sqrt{\pi}}\zeta^2 \exp(-\zeta^2) & \text{if } x < 0, \\ \dfrac{2}{\sqrt{\pi}}\zeta^2 \exp(-\zeta^2) & \text{if } x > 0, \end{cases} \\ f_1^{ini}(x,\zeta) = 0, \end{cases}$$

for (x,ζ) in $[-10:10] \times [0,6]$. The non constant electric field and collisional parameter are given by

$$E(x) = \exp(-|x|), \qquad \alpha_{ei}(x) = \mathrm{A} \cdot (\arctan(1 + 0.5 \cdot x) + \arctan(1 - 0.5 \cdot x),$$

where the constant A will be specified hereafter. Neumann boundary conditions are considered and we take $\Delta x = \Delta\zeta = 10^{-1}$ and the modulus energy

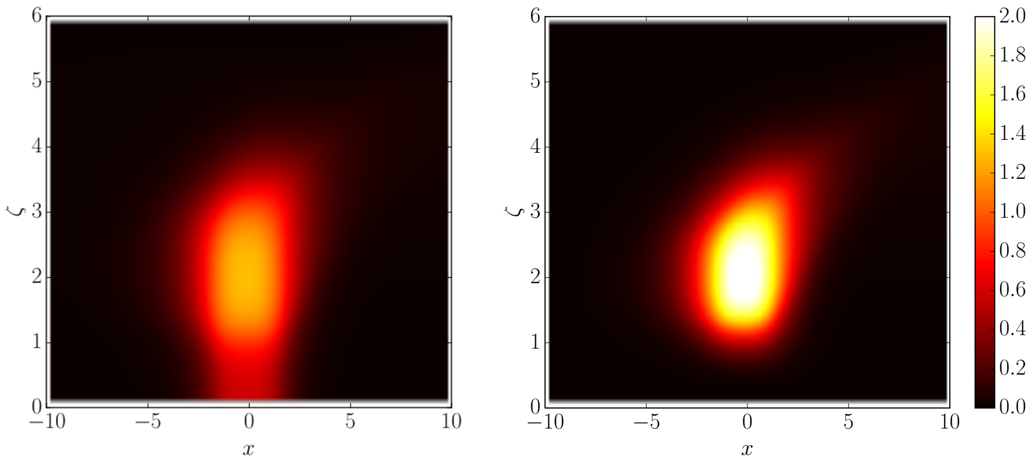

Figure 9: Test 1c : representation of the f_0 profile obtained with the HLL scheme (left) and the asymptotic-preserving scheme (right) at time $t = 100$ in the case of a non constant collisional parameter.

step to 10^{-1}. We define the electronic density n by

$$n(x) = \int_0^{+\infty} f_0(x, \zeta) d\zeta.$$

Fig. 10 shows the electronic density profiles obtained with the second-order HLL and asymptotic-preserving schemes at different times and for different values of A. For A = 1 corresponding to a weak collisional regime, we observe that HLL and asymptotic-preserving schemes are really close. On the contrary, as noticed in the previous test case, in strong collisional regimes, the results obtained with the HLL scheme are much more diffused that the ones obtained with the asymptotic-preserving scheme. Indeed, in the case A $= 10^4$ it is observed that the profile obtained with the asymptotic-preserving scheme is very close to the one obtained with the diffusion scheme while the second order HLL scheme is not accurate.

7 Conclusion

In this work, a new asymptotic-preserving scheme has been proposed for the electronic M_1 model. It is based on a very simple modification of the HLL scheme in order to capture the correct asymptotic limit in the diffusive limit. This modification also ensures the admissibility of the numerical solution under suitable CFL conditions. The new scheme has also been understood as a Godunov-type scheme based on a given approximate Riemann solver. Several numerical test cases have been proposed to show the relevance of

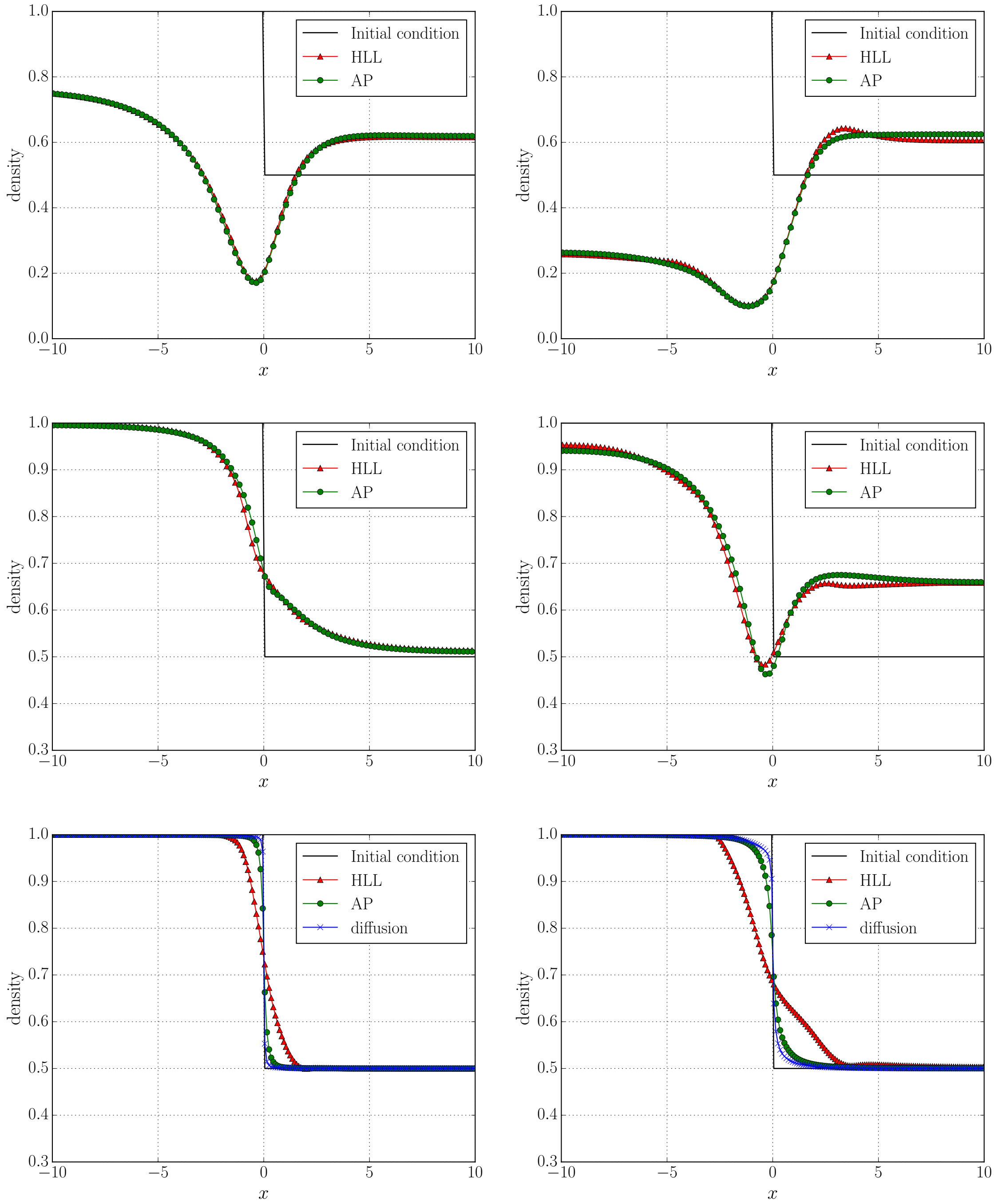

Figure 10: Test 2 : representation of the density profiles obtained with the HLL scheme (red), with the AP scheme (green) and with the diffusion scheme (blue) at time $t = 50$ (left) and $t = 400$ (right) for $\mathrm{A} = 1$ (top), $\mathrm{A} = 10^2$ (middle) and $\mathrm{A} = 10^4$ (bottom).

the proposed scheme in different regimes.
Considering the perpectives of this work, we would like to provide a rigorous analysis of the proposed second-order type extension. We are also interested in considering the contribution of an electron-electron collision operator and the coupling with the Maxwell-Ampere equation.

References

[1] G.W. Alldredge, C.D. Hauck, and A.L. Tits. High-order entropy-based closures for linear transport in slab geometry II: A computational study of the optimization problem. SIAM Journal on Scientific Computing Vol. 34-4 (2012), pp. B361-B391.

[2] D. Aregba-Driollet, M. Briani, and R. Natalini. Asymptotic High-Order Schemes for 2x2 Dissipative Hyperbolic Systems. SIAM Journal on Numerical Analysis 46 (2008), 869-894.

[3] M. Ben-Artzi and J. Falcovitz. Generalized Riemann problems in computational fluid dynamics. Cambridge University Press. G (Vol. 11), (2003).

[4] C. Berthon, P. Charrier, and B. Dubroca. An asymptotic preserving relaxation scheme for a moment model of radiative transfer. C. R. Acad. Sci. Paris, Ser. I 344 (2007).

[5] C. Berthon, P. Charrier, and B. Dubroca. An HLLC Scheme to Solve The M1 Model of Radiative Transfer in Two Space Dimensions. Journal of Scientific Computing, Vol. 31, No. 3, (2007).

[6] C. Berthon and R.Turpault. Asymptotic preserving HLL schemes. Numerical Methods for Partial Differential Equations, 27 (6) (2011) 1396-1422.

[7] F. Blachère and R. Turpault. An asymptotic-preserving scheme for systems of conservation laws with source term on 2D unstructured meshes with high-order MOOD reconstruction. F. Blachère and R. Turpault., to appear in Comput. Methods Appl. Mech. Engrg. (2017).

[8] S. Boscarino, P.G. LeFloch, and G. Russo. High-order asymptotic-preserving methods for fully nonlinear relaxation problems. SIAM J. Sci. Comput. Vol. 36, No.2, pp.A377-A395.

[9] F. Bouchut. Nonlinear Stability of Finite Volume Methods for Hyperbolic Conservation Laws, and Well-Balanced Schemes for sources. Frontiers in Mathematics series, Birkhauser. (2004).

[10] F. Bouchut, H. Ounaissa, and B. Perthame. Upwinding of the source term at interfaces for Euler equations with high friction. Computers and Mathematics with Applications 53 (2007), 361-375.

[11] C. Buet and S. Cordier. Conservative and entropy decaying numerical scheme for the isotropic Fokker-Planck-Landau equation. J. Comput. Phys. 145, No.1, 228-245 (1998).

[12] C. Buet and B. Després. Asymptotic preserving and positive schemes for radiation hydrodynamics. J. Compt. Phy., 215, 717–740 (2006).

[13] C. Chalons, F. Coquel, E. Godlewski, P.-A. Raviart, and N. Seguin. Godunov-type schemes for hyperbolic systems with parameter-dependent source. The case of Euler system with friction. Math. Models Methods Appl. Sci. 20 (2010), no. 11, 2109–2166. MR 2740716 (2011m:65179).

[14] C. Chalons, M. Girardin, and S. Kokh. An all-regime Lagrange-Projection like scheme for 2D homogeneous models for two-phase flows on unstructured meshes. Journal of Computational Physics. 335, pp. 885-904 (2017).

[15] C. Chalons, M. Girardin, and S. Kokh. An all-regime Lagrange-Projection like scheme for the gas dynamics equations on unstructured meshes. Communications in Computational Physics (CICP), Vol. 20, No. 1, pp. 188-233 (2016).

[16] C. Chalons, M. Girardin, and S. Kokh. Operator-splitting-based asymptotic-preserving scheme for the gas dynamics equations with stiff source terms. Proceedings of the 2012 International Conference on Hyperbolic Problems: Theory, Numerics, Applications.

[17] G Dimarco and L Pareschi. Asymptotic Preserving Implicit-Explicit Runge–Kutta Methods for Nonlinear Kinetic Equations. SIAM Journal on Numerical Analysis 51 (2013), 1064-1087.

[18] B. Dubroca, J.-L. Feugeas, and M. Frank. Angular moment model for the Fokker-Planck equation. European Phys. Journal D, 60, 301, (2010).

[19] B. Dubroca and J.L. Feugeas. Étude théorique et numérique d'une hiéarchie de modèles aux moments pour le transfert radiatif. C. R. Acad. Sci. Paris, t. 329, SCrie I, p. 915-920, (1999).

[20] F. Filbet and S. Jin. A class of asymptotic preserving schemes for kinetic equations and related problems with stiff sources. J. Comp. Phys. vol. 229, no 20 (2010).

[21] L. Gosse. Computing qualitatively correct approximations of balance laws. SEMA SIMAI Springer Series.

[22] L. Gosse and G. Toscani. An asymptotic-preserving well-balanced scheme for the hyperbolic heat equations. C. R. Math. Acad. Sci. Paris 334 (4) (2002) 337–342.

[23] L. Gosse and G. Toscani. Space localizaion and well-balanced schemes for discrete kinetic models in diffusive regimes. SIAM J. Numer. Anal. 41 (2) (2003) 641–658.

[24] C.P.T. Groth and J.G. McDonald. Towards physically-realizable and hyperbolic moment closures for kinetic theory. Continuum Mech. Thermodyn. 21, 467-493 (2009).

[25] S. Guisset, S. Brull, E. d'Humières, and B. Dubroca. Asymptotic-preserving well-balanced scheme for the electronic M_1 model in the diffusive limit: particular cases. To appear in ESAIM: Mathematical Modelling and Numerical Analysis. DOI: http://dx.doi.org/10.1051/m2an/2016079.

[26] S. Guisset, S. Brull, B. Dubroca, E. d'Humières, S. Karpov, and I. Potapenko. Asymptotic-preserving scheme for the Fokker-Planck-Landau-Maxwell system in the quasi-neutral regime. Communications in Computational Physics, volume 19, issue 02, pp. 301-328 (2016).

[27] S. Guisset, S. Brull, B. Dubroca, and R. Turpault. Asymptotic-preserving for the electronic M_1 model in the diffusive limit. Submitted.

[28] S. Guisset, S. Brull, E. d'Humières, B. Dubroca, and V. Tikhonchuk. Classical transport theory for the collisional electronic M1 model. Physica A: Statistical Mechanics and its Applications, Volume 446, Pages 182-194 (2016).

[29] A. Harten, P.D. Lax, and B. Van Leer. On upstream differencing and Godunov-type schemes for hyperbolic conservation laws. SIAM Review 25 (1983), 35-61.

[30] S. Jin and C.D. Levermore. Fully discrete numerical transfer in diffusive regimes. Transport Theory Statist. Phys. 22 (6) 739–791. (1993).

[31] S. Jin and C.D. Levermore. The discrete-ordinate method in diffusive regimes. Transport Theory Statist. Phys. 20 (5–6) 413–439. (1991).

[32] P. Lafitte and G. Samaey. Asymptotic-preserving projective integration schemes for kinetic equations in the diffusion limit. SIAM Journal on Scientific Computing , 34(2):A579– A602, 2012.

[33] B. Van Leer. Towards the ultimate conservative difference scheme III. Upstream-centered finite-difference schemes for ideal compressible flow. J. Comput. Phys. 23, 3 (Mar. 1977), 263–275.

[34] M. Lemou and L. Mieussens. A new asymptotic preserving scheme based on Micro-Macro formulation for linear kinetic equations in the diffusion limit. SIAM J. Sci. Comput., 31(1), 334–368, 2008.

[35] C.D. Levermore. Moment closure hierarchies for kinetic theories. J. Stat. Phys. 83, 1021-1065 (1996).

[36] J. Mallet, S. Brull, and B. Dubroca. An entropic scheme for an angular moment model for the classical Fokker-Planck-Landeau equation of electrons. Comm. Comput. Phys., 422, (2013).

[37] J.G. McDonald and C.P.T. Groth. Towards realizable hyperbolic moment closures for viscous heat-conducting gas flows based on a maximum-entropy distribution. Continuum Mech. Thermodyn. 25, 573-603 (2012).

[38] G.N. Minerbo. Maximum entropy Eddigton Factors. J. Quant. Spectrosc. Radiat. Transfer, 20, 541, (1978).

[39] I. Muller and T. Ruggeri. Rational Extended Thermodynamics. Springer, New York (1998).

[40] Ph. D. Nicolai, J.-L. A. Feugeas, and G. P. Schurtz. A practical nonlocal model for heat transport in magnetized laser plasmas. Phys. Plasmas 13, 032701, (2006).

[41] G.C. Pomraning. Maximum entropy Eddington factors and flux limited diffusion theory. J. of Quantitative Spectroscopy and Radiative Transfer, 26 5 385-388 (1981).

[42] L. Spitzer and R. Härm. Phys. Rev. 89 (1953) 977.

[43] H. Struchtrup. Macroscopic Transport Equations for Rarefied Gas Flows. Springer, Berlin (2005).

[44] R. Turpault. A consistent multigroup model for radiative transfer and its underlying mean opacity. J. Quant. Spectrosc. Radiat. Transfer 94, 357–371 (2005).